Rapid Communications

Wiedemann-Franz law in a non-Fermi liquid and Majorana central charge: Thermoelectric transport in a two-channel Kondo system

Gerwin A. R. van Dalum,[1] Andrew K. Mitchell,[2] and Lars Fritz[1]
[1]*Institute for Theoretical Physics, Utrecht University, Princetonplein 5, 3584 CC Utrecht, Netherlands*
[2]*School of Physics, University College Dublin, Belfield, Dublin 4, Ireland*

(Received 25 December 2019; revised 22 June 2020; accepted 23 June 2020; published 8 July 2020)

Quantum dot devices allow one to access the critical point of the two-channel Kondo model. The effective critical theory involves a free Majorana fermion quasiparticle localized on the dot. As a consequence, this critical point shows both the phenomenon of non-Fermi-liquid physics and fractionalization. Although a violation of the Wiedemann-Franz law is often considered to be a sign of non-Fermi-liquid systems, we show by exact calculations that it holds at the critical point, thereby providing a counterexample to this lore. Furthermore, we show that the fractionalized Majorana character of the critical point can be unambiguously detected from the heat conductance, opening the door to a direct experimental measurement of the elusive Majorana central charge $c = \frac{1}{2}$.

DOI: 10.1103/PhysRevB.102.041111

Originally conceived to understand the behavior of magnetic impurities in metals [1], the single-channel Kondo model also successfully describes simple quantum dot devices [2–4] and their low-energy Fermi-liquid (FL) behavior [5]. Such circuit realizations of fundamental quantum impurity models are exquisitely tunable and allow the nontrivial dynamics of strongly correlated electron systems to be probed experimentally through quantum transport. The FL properties of such systems, as well as their bulk counterparts, are evidenced by their low-temperature thermoelectric transport, which satisfies the Wiedemann-Franz (WF) law [6,7]. Conversely, violations of the WF law are observed in various systems with non-Fermi-liquid (NFL) properties [8–17].

Another advantage of nanoelectronics devices incorporating quantum dots is that more exotic states of quantum matter can be engineered. In particular, there has been considerable interest recently, from both theory and experiment, in *multichannel* Kondo systems [18] which exhibit NFL quantum critical physics due to frustrated Kondo screening, and the emergence of non-Abelian anyonic quasiparticles [19–21]. The NFL two-channel Kondo (2CK) critical point, realized experimentally in Refs. [22–24], is described by an effective theory involving Majorana fermions [25], while the three-channel Kondo (3CK) critical point realized in Ref. [26] involves Fibonacci anyons [21]. This NFL character and the fractionalization is most clearly seen in the dot entropy of $S = k_B \ln(\sqrt{2})$ for 2CK and $k_B \ln(\phi)$ for 3CK (with ϕ the golden ratio). However, the experimental quantity measured up until now in 2CK and 3CK devices has been the charge conductance [22,23,27,28]. In particular, recent charge-Kondo implementations demonstrate precise quantitative agreement between theoretical predictions and experimental measurements for the entire universal scaling curves [24,26,29,30]. This confirms the underlying theoretical description, but as yet there is no *direct* experimental evidence of either the NFL character or the fractionalization in these systems.

Thermoelectric transport in multichannel Kondo systems is far less well understood. In this Rapid Communication, we present exact analytic results for heat transport in the charge-2CK (C2CK) setup depicted in Fig. 1, relevant to recent experiments [24]. Our choice of system is motivated by the unprecedented control in such a device to probe the NFL critical point; our theoretical predictions are within reach of existing experiments. The C2CK setup allows the WF law [6] to be studied at an exactly solvable NFL critical point. A violation of the WF law has often been used as an empirical rule of thumb to identify NFL physics [8–14]. Nevertheless, we explicitly find that it is satisfied at the charge-2CK NFL critical point. Furthermore, as shown below, the heat conductance is a universal quantity in the critical C2CK system (unlike in the standard spin-2CK implementation), and provides a route to measure experimentally the Majorana central charge.

We emphasize that we study the nonperturbative regime where both source and drain leads are strongly coupled to the dot (although we focus on linear response corresponding to a small voltage bias and temperature gradient). For this setup, the numerical renormalization group [31] (usually considered to be the numerical method of choice for solving generalized quantum impurity problems) cannot be used to calculate heat transport.

Charge 2CK setup, model, and observables. Figure 1 shows schematically the C2CK system studied experimentally in Ref. [24]. Reference [30] demonstrated that this quantum dot device realizes an essentially perfect experimental quantum simulation of the C2CK model of Matveev [29], by comparing experimental data for charge conductance with numerical renormalization group calculations. Here, we compute exact thermoelectric transport analytically at the 2CK critical point for the same model.

The key ingredient required to realize 2CK physics is ensuring that the two leads constitute two distinct, independent channels (not mixed by interchannel charge transfer). This is achieved in the C2CK device by exploiting a mapping

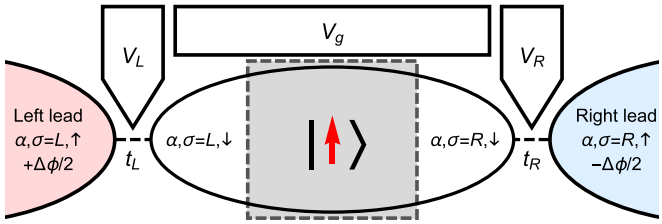

FIG. 1. Schematic of the C2CK device. Gate voltages $V_{L,R}$ govern the transmission coefficients $t_{L,R}$ at the left and right quantum point contacts, while V_g controls the dot charge. Coherent transport across the dot is suppressed by the intervening ohmic contact. Thermoelectric transport is measured in response to a potential difference $\Delta\phi$ (voltage bias or temperature gradient). A spinless system at the dot charge degeneracy point maps to a 2CK model.

between charge and (pseudo)spin states [29]. The physical system is effectively spinless (due to the application of a large polarizing magnetic field), and a large dot is tuned to a step in its Coulomb-blockade staircase (using gate voltage V_g), such that dot charge states with N and $N+1$ electrons are degenerate. Regarding this pair of macroscopic dot charge states as a pseudospin (such that $\hat{S}^+ = |N+1\rangle\langle N|$ and $\hat{S}^- = (S^+)^\dagger$) and simply relabeling dot electrons as "down" spin, and lead electrons as "up" spin, yields a 2CK pseudospin model—provided there is no coherent transport between electronic systems around each quantum point contact (QPC). In practice, this is achieved by placing an ohmic contact (metallic island) on the dot to separate the channels [24] (gray box in Fig. 1). The resulting C2CK Hamiltonian reads

$$H_{\rm K} = \sum_{\alpha=L,R}\Bigg[\sum_k(\epsilon_{\alpha\uparrow k}c^\dagger_{\alpha\uparrow k}c_{\alpha\uparrow k}+\epsilon_{\alpha\downarrow k}c^\dagger_{\alpha\downarrow k}c_{\alpha\downarrow k}) + t_\alpha\sum_{k,k'}(c^\dagger_{\alpha\uparrow k}c_{\alpha\downarrow k'}\hat{S}^- + c^\dagger_{\alpha\downarrow k}c_{\alpha\uparrow k'}\hat{S}^+)\Bigg] + \Delta E\hat{S}^z, \quad (1)$$

where $c_{\alpha\sigma k}$ are electronic operators, and $\alpha = L, R$ denotes whether the electron resides to the left or right of the gray metallic island in Fig. 1. The label σ describes whether the electron lives in the leads ($\uparrow$) or on the dot ($\downarrow$). The effective continuum of states on the large dot is characterized by the dispersion $\epsilon_{\alpha\downarrow k}$, while the leads have dispersion $\epsilon_{\alpha\uparrow k}$. The term $\Delta E\hat{S}^z$ describes detuning away from the dot charge degeneracy point, which acts as a pseudospin field. Equation (1) is a maximally spin-anisotropic version of the regular spin-2CK model [18]. A major advantage of this setup over the conventional spin-2CK paradigm is that the pseudospin "exchange" coupling in the effective model is simply related to the QPC transmission, and can be large. In turn this means that the 2CK Kondo temperature $T_{\rm K}$ can be high, and hence the critical point is comfortably accessible at experimental base temperatures [24]. The critical point arises for $\Delta E = 0$ and $\sqrt{\nu_{L\uparrow}\nu_{L\downarrow}}t_L = \sqrt{\nu_{R\uparrow}\nu_{R\downarrow}}t_R$, where $\nu_{\alpha\sigma}$ is the Fermi-level density of states of channel $\alpha\sigma$ (in turn related to the dispersions $\epsilon_{\alpha\sigma k}$). This condition can be achieved [24] by tuning the gate voltages V_g, V_L, and V_R (Fig. 1).

We now consider applying a voltage bias ΔV, and/or temperature gradient ΔT, between the left and right leads. The thermoelectric transport coefficients are determined from the resulting charge current I_c and heat current I_Q,

$$\begin{pmatrix} I_c \\ I_Q \end{pmatrix} = \begin{pmatrix} \chi_{cc} & \chi_{cQ} \\ \chi_{Qc} & \chi_{QQ} \end{pmatrix}\begin{pmatrix} \Delta V \\ \Delta T/T \end{pmatrix}, \quad (2)$$

where $I_{c,Q} \equiv \langle\hat{I}_{c,Q}\rangle$. The current operators are given by

$$\hat{I}_c = \frac{e}{2}\frac{d}{dt}(N_{L,\uparrow}-N_{R,\uparrow}) = -\frac{ie}{2\hbar}[N_{L,\uparrow}-N_{R,\uparrow},H],$$
$$\hat{I}_Q = \frac{i}{2\hbar}[H_{L,\uparrow}-H_{R,\uparrow}-\mu(N_{L,\uparrow}-N_{R,\uparrow}),H]. \quad (3)$$

With $I_c = G\Delta V$ defined at $\Delta T = 0$, and $I_Q = \kappa\Delta T$ defined at $I_c = 0$, we wish to calculate the charge conductance $G = \chi_{cc}$ and heat conductance $\kappa = (\chi_{QQ} - \chi_{Qc}\chi_{cQ}/\chi_{cc})/T$.

The charge and heat conductances in linear response can be obtained from the Kubo formula in terms of equilibrium current-current correlation functions [32,33],

$$\chi_{ij} = \lim_{\omega\to 0}\frac{-\mathrm{Im}\,K_{ij}(\omega,T)}{\hbar\omega}, \quad (4)$$

where $i, j = c, Q$, and $K_{ij}(\omega, T)$ is the Fourier transform of the retarded autocorrelator $K_{ij}(t,T) = -i\theta(t)\langle[\hat{I}_i(t),\hat{I}_j(0)]\rangle$.

Emery-Kivelson effective model. A generalized version of the 2CK model can be solved exactly at a special point in its parameter space, corresponding to a specific value of the exchange anisotropy [25]. The C2CK model Eq. (1) (as well as the regular spin-2CK model) does not satisfy this condition. The complete renormalization group (RG) flow and full conductance line shapes at this Emery-Kivelson (EK) point are therefore different from those of the physical system of interest. However, spin anisotropy is RG irrelevant in the 2CK model [19,20,34], meaning that the same spin-isotropic critical point is reached asymptotically at low temperatures, independently of any anisotropy in the bare model. The EK solution can therefore be used to understand the NFL critical fixed point of the C2CK system [35,36]. This approach has been validated for the entire NFL to FL crossover arising due to small symmetry-breaking perturbations in Refs. [28,30] and we adopt the same strategy.

After bosonization, canonical transformation, and refermionization, the EK effective model reads [25]

$$H = \sum_\nu\sum_k\epsilon_k\psi^\dagger_{\nu,k}\psi_{\nu,k} + g_\perp[\psi^\dagger_{sf}(0)+\psi_{sf}(0)](d^\dagger - d) + \frac{\Delta E}{2}(d^\dagger d - dd^\dagger), \quad (5)$$

where $\psi_{\nu,k}$ (with $\nu = c, s, f, sf$) are effective lead fermion fields, and the impurity spin is parametrized by a fermionic operator $d = i\hat{S}^+$. For all further calculations, we set $\epsilon_k = \hbar v_F k$ for the full range of k, where v_F is the Fermi velocity. As a result of the mapping, the effective model takes the form of a noninteracting Majorana resonant level at the critical point $\Delta E = 0$. We introduce Majorana operators,

$$\hat{a} = (d^\dagger + d)/\sqrt{2} \quad \text{and} \quad \hat{b} = (d^\dagger - d)/i\sqrt{2}, \quad (6)$$

such that $\{\hat{a},\hat{a}\} = \{\hat{b},\hat{b}\} = 1$ and $\{\hat{a},\hat{b}\} = 0$. The effective theory, Eq. (5), successfully accounts for the residual fractional dot entropy at the C2CK critical point, arising from the strictly decoupled $\hat{a}$ Majorana.

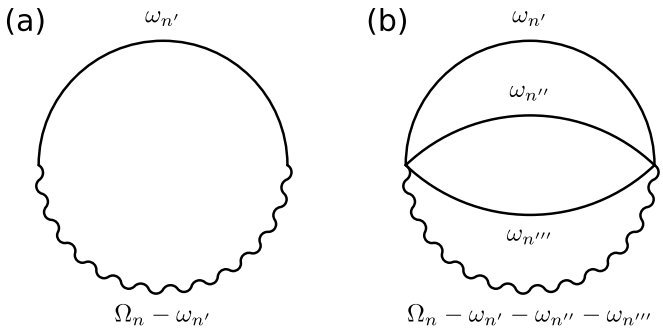

FIG. 2. The only Feynman diagrams contributing to (a) the charge conductance G, and (b) the heat conductance κ. Ω_n represents the external bosonic Matsubara frequency, and we sum over the remaining fermionic Matsubara frequencies ω_n.

A remarkable feature of the EK mapping is that it holds even with a finite voltage bias between leads, allowing charge transport to be calculated beyond linear response [37]. However, this approach cannot be used for nonequilibrium transport in the presence of a temperature difference between the leads because the EK mapping mixes the two electronic baths, and so the EK channels cannot be assigned a definite temperature. In the following, we therefore confine attention to thermoelectric transport in linear response using the Kubo formula [32].

Current operators in the EK basis. Transforming the charge and heat current operators, Eq. (3), into the EK basis and writing in terms of dot Majorana operators $\hat{a}$ and $\hat{b}$ from Eq. (6), we find

$$\hat{I}_c = \frac{e g_\perp}{\sqrt{2L}\hbar} \sum_k (\psi^\dagger_{sf,k} - \psi_{sf,k})\hat{b}, \tag{7}$$

for the charge current, but for the heat current,

$$\begin{aligned}\hat{I}_Q = {} & \frac{i\pi v_F g_\perp}{(2L)^{3/2}} \sum_{k,k',k''} (2\,\psi^\dagger_{f,k'}\psi_{f,k''} + \delta_{k',k''})(\psi^\dagger_{sf,k} + \psi_{sf,k})\hat{a} \\ & - \frac{\pi v_F g_\perp}{\sqrt{2}L^{3/2}} \sum_{k,k',k''} (\psi^\dagger_{c,k'}\psi_{c,k''} + \psi^\dagger_{s,k'}\psi_{s,k''})(\psi^\dagger_{sf,k} - \psi_{sf,k})\hat{b} \\ & + \frac{\pi v_F}{2L} \sum_{k,k'} (\epsilon_{k'} - \epsilon_k)(\psi^\dagger_{f,k}\psi_{f,k'} + \psi^\dagger_{sf,k}\psi_{sf,k'})\hat{a}\hat{b}. \end{aligned} \tag{8}$$

Here, L is the length of a lead, and we have set $\mu = 0$.

Linear response coefficients. The calculation of the charge conductance G is rather straightforward [37], involving as it does only one-loop Feynman diagrams of the type shown in Fig. 2(a). Here, we represent diagrammatically the local (imaginary time) bare bath propagators $L^0_\nu(\tau) = -1/L \sum_k \langle \hat{T}\psi_{\nu,k}(\tau)\psi^\dagger_{\nu,k}(0)\rangle_0$ (with $\nu = c, s, f, sf$) using "straight" lines, while the fully renormalized Majorana Green's function $D_{bb}(\tau) = \langle \hat{T} b(0)b(\tau)\rangle$ is represented diagrammatically as a "wiggly" line. For more details on the calculation and the definition of the Green's function, see the Supplemental Material [35].

At the critical point, the EK calculation yields the well-known leading order in temperature result for the charge conductance [30,37],

$$G = \frac{e^2}{2h}. \tag{9}$$

By contrast, the heat conductance calculation is far more involved. In this case, one must compute three-loop Feynman diagrams of the type shown in Fig. 2(b). After a lengthy calculation [35], we find the following form for the leading-order low-temperature heat conductance,

$$\kappa = \frac{\pi^2 k_B^2 T}{6h}, \tag{10}$$

and the off-diagonal components $\chi_{cQ} = \chi_{Qc}$ vanish. These are exact results at the critical point of the C2CK system. Equation (10) is our central result, the physical consequences of which are explored in detail in the following.

Applicability of the EK solution. The leading-order finite-temperature corrections to Eqs. (9) and (10) are linear in T. They originate from the leading irrelevant operator, of scaling dimension 3/2, which is $H_I = \frac{i\lambda}{L}\hat{b}\hat{a}\sum_{k,k'} : \psi^\dagger_{s,k}\psi_{s,k'} :$ [25], corresponding to spin anisotropy. In the Supplemental Material [35] we show that this implies $G = \frac{e^2}{2h}(1 - \frac{\pi^3\lambda^2}{8h^2v_F^2}\frac{T}{T_K} + \cdots)$, where T_K is the Kondo temperature. A similar calculation for the heat conductance is five-loop, which we did not attempt. However, the structure of the perturbation theory implies a similar generic form, $\kappa = \frac{\pi^2 k_B^2 T}{6h}(1 - b\lambda^2\frac{T}{T_K} + \cdots)$. Both G and κ are *finite* at the EK point, with leading corrections controlled by powers of T/T_K which vanish at the critical C2CK fixed point as $T/T_K \to 0$.

Wiedemann-Franz law. For weakly interacting metals, Wiedemann and Franz found [6] a remarkable relation between the low-temperature electrical and thermal conductivities: $\lim_{T/T_F\to 0}\kappa/(T\sigma) = L_0$, where $L_0 = \pi^2 k_B^2/3e^2$ is the Lorenz number which involves only fundamental constants and T_F is the Fermi temperature (the relation is asymptotic, based on a leading-order expansion in T/T_F). Metals are good conductors of both charge and heat, since the carriers in both cases are itinerant electrons. Such a relation also holds in the context of many nanoelectronics systems at low temperatures (where the conductance G plays the role of σ), even with strong electronic correlations [7]—provided the system is a Fermi liquid at low temperatures. Indeed, a violation of the WF law is often considered a hallmark of non-Fermi-liquid physics, since there the carriers are not simply bare electrons or "dressed" fermionic quasiparticles as in FL theory, but more complicated objects, possibly with different and even fractionalized quantum numbers.

The C2CK system offers a rare opportunity to test the WF law at an exactly solvable NFL critical point, and to make a concrete prediction for experiments. Interestingly—and contrary to conventional expectation—we find that the WF law is *satisfied* at the C2CK NFL critical point,

$$\lim_{T/T_K\to 0} \frac{\kappa}{TG} = \frac{\pi^2 k_B^2}{3e^2}. \tag{11}$$

Since G and κ are both finite at the C2CK critical fixed point, and corrections to the fixed point are strictly RG irrelevant, Eq. (11) is exact.

The WF law is expected to be *violated* in the FL phase of the C2CK model. After preparing the C2CK system at the NFL critical point, consider introducing a small symmetry-breaking perturbation (coupling the dot more strongly to one lead than the other). The system flows under RG on further reducing temperature to a Fermi-liquid state, in which the dot pseudospin is fully Kondo screened by one lead, while the other asymptotically decouples [29]. The resulting charge conductance $G \to 0$ in the FL phase [30], since one of the two physical leads involved in transport decouples. For the same reasons, $\kappa/T \to 0$. The WF ratio, obtained in the limiting process of $T/T_K \to 0$, is therefore expected to take a nonuniversal value with a different Lorenz ratio $L \neq L_0$ due to the leading temperature-dependent corrections to the FL fixed point values of G and κ.

Measuring the Majorana central charge. The EK effective model for the C2CK system is essentially a one-dimensional (1D) boundary problem. Critical systems in 1D are described by conformal field theories in $1+1$ dimensions, as characterized by the so-called conformal charge c. Recently, it was conjectured that heat transport is directly proportional to the conformal charge of the underlying conformal field theory [38]. For translationally invariant critical systems with left and right leads held at temperatures T_L and T_R, the heat current is given by $I_Q = \pi^2 k_B^2 c(T_L^2 - T_R^2)/6h$. Within linear response, we take $T_R = T$ and $T_L = T + \Delta T$, and expand to leading order in ΔT,

$$I_Q = \frac{\pi^2 k_B^2}{3h} cT\,\Delta T + \mathcal{O}[(\Delta T)^2], \tag{12}$$

which allows us to identify κ as

$$\kappa = \frac{\pi^2 k_B^2}{3h} cT. \tag{13}$$

Comparing this to Eq. (10), we find that the central charge of the underlying effective critical theory is $c = \frac{1}{2}$. This is consistent with the known result of $c = \frac{1}{2}$ for one-dimensional Majorana fermions in the unitary limit [20]. We argue that heat transport measurements therefore provide clear experimental access to the fractionalized nature of the excitations in the C2CK system.

Comparison with spin-2CK. The above results are specific to the C2CK setup relevant to recent experiments [24,26]. Here, we briefly contrast to the standard spin-2CK setup of Refs. [22,23], in which one of the two conduction electron channels is "split" into source and drain leads, with their hybridization to the quantum dot parametrized by Γ_s and Γ_d, respectively (the other channel is a Coulomb-blockaded quantum box). Although the effective EK model at the 2CK critical point is the same, the form of the current operators [the analog of Eqs. (7) and (8)] is obviously different. Indeed, the "proportionate coupling" geometry of that setup affords a significant simplification, with charge and heat conductances expressible simply in terms of the scattering t-matrix spectrum $t(T,\omega)$ as shown in Ref. [7]. At the spin-2CK critical fixed point, the charge conductance for $T/T_K \to 0$ follows as $G = 2\gamma e^2 t(0,0)/h$, while the heat conductance is $\kappa = 2\gamma\pi^2 k_B^2 T t(0,0)/3h$, where the geometrical factor is $\gamma = 4\Gamma_s\Gamma_d/(\Gamma_s+\Gamma_d)^2$, and at the 2CK fixed point we have [20,28] $t(0,0) = \frac{1}{2}$. The spin-2CK conductances are therefore not universal and depend on system geometry through γ. There is no interpretation in terms of the central charge since the setup is not a translationally invariant 1D system. On the other hand, the WF law is satisfied since $L = \kappa/TG = \pi^2 k_B^2/3e^2 = L_0$. In this setup, channel asymmetry produces a flow away from the NFL critical point and towards a low-temperature FL state, in which the leads probing transport can be either in strong coupling (SC) or weak coupling (WC) with the dot (depending on which channel couples more strongly). At SC, $t(0,0) = 1$ and the WF law is again satisfied. However, at WC, $t(0,0) = 0$ and the leading (quadratic) Fermi-liquid corrections to the t matrix must be considered [28]. In this case we find a different universal ratio $L = 7\pi^2 k_B^2/5e^2 \neq L_0$. A similar analysis can be performed for the spin-3CK situation [39], where the NFL fixed point is characterized by $t(0,0) = \cos(2\pi/5)$.

Failure of NRG for heat transport via Kubo. Finally, we comment that our exact analytic results for heat conductance in the C2CK system are, perhaps surprisingly, *inaccessible* with the numerical renormalization group [31] (NRG). If a system satisfies "proportionate coupling," thermoelectric transport coefficients may be related to moments of the scattering t matrix, and NRG can be used to obtain accurate results, as demonstrated in Refs. [7,40] for the Anderson model. However, the geometry of the setup depicted in Fig. 1 does not admit any such formulation of the conductances in terms of the t matrix, and one must fall back on the Kubo formula, Eq. (4). The latter uses the heat current operator Eq. (3), which involves the lead Hamiltonian $H_{\alpha,\uparrow}$. In NRG, a specific discretized form of $H_{\alpha,\uparrow}$ is used, but these "Wilson chains" do not act as proper thermal reservoirs [41]. We find that exact FL results for even the simple resonant level model cannot be reproduced with the Kubo formula when Wilson chains are used for leads. NRG can of course be used to compute impurity dynamical quantities or the t matrix [31], and the Kubo formula may still be used for charge transport within NRG [26,30,42,43].

Conclusions and outlook. We studied charge and heat transport in the C2CK system recently realized experimentally [24], by exploiting the exact solution of the related EK model [25] and RG arguments. In particular, our result for the low-temperature heat conductance at the NFL critical point, $\kappa = \pi^2 k_B^2 T/6h$, is exact. Our results show that the WF law is satisfied, despite being a NFL. Furthermore, we demonstrate that the heat transport provides an experimental route to determine the central charge of the underlying conformal field theory, which in this case is $c = \frac{1}{2}$ because an effective Majorana fermion mediates charge and heat transport through the dot. It would be interesting to extend this study to the charge-3CK system in the regime where all leads are coupled nonperturbatively. This is a formidable theoretical challenge since there is no equivalent exact solution available as with C2CK, and one should expect WF to be violated. We note that heat transport measurements in a C3CK system are within existing experimental reach [26].

Note added. Recently, we became aware of Ref. [44], which considers the closely related problem of thermoelectric transport in a three-channel charge Kondo problem with an additional weakly coupled probe lead.

Acknowledgments. We thank P. Simon and E. Sela for helpful discussions. L.F. and G.D. acknowledge funding from the D-ITP consortium, a program of the Netherlands Organisation for Scientific Research (NWO) that is funded by the Dutch Ministry of Education, Culture and Science (OCW). A.K.M. acknowledges funding from the Irish Research Council Laureate Awards through Grant No. IRCLA/2017/169.

[1] A. C. Hewson, *The Kondo Problem to Heavy Fermions* (Cambridge University Press, Cambridge, U.K., 1997).
[2] D. Goldhaber-Gordon, H. Shtrikman, D. Mahalu, D. Abusch-Magder, U. Meirav, and M. A. Kastner, Nature (London) **391**, 156 (1998).
[3] S. M. Cronenwett, T. H. Oosterkamp, and L. P. Kouwenhoven, Science **281**, 540 (1998).
[4] M. Pustilnik and L. Glazman, J. Phys.: Condens. Matter **16**, R513 (2004).
[5] P. Nozières, J. Low Temp. Phys. **17**, 31 (1974).
[6] R. Franz and G. Wiedemann, Ann. Phys. **165**, 497 (1853).
[7] T. A. Costi and V. Zlatić, Phys. Rev. B **81**, 235127 (2010).
[8] R. Scheibner, H. Buhmann, D. Reuter, M. N. Kiselev, and L. W. Molenkamp, Phys. Rev. Lett. **95**, 176602 (2005).
[9] A. Garg, D. Rasch, E. Shimshoni, and A. Rosch, Phys. Rev. Lett. **103**, 096402 (2009).
[10] R. Mahajan, M. Barkeshli, and S. A. Hartnoll, Phys. Rev. B **88**, 125107 (2013).
[11] R. Žitko, J. Mravlje, A. Ramšak, and T. Rejec, New J. Phys. **15**, 105023 (2013).
[12] J. Zaanen, Y. Liu, Y.-W. Sun, and K. Schalm, *Holographic Duality in Condensed Matter Physics* (Cambridge University Press, Cambridge, U.K., 2015).
[13] T. K. T. Nguyen and M. N. Kiselev, Phys. Rev. B **97**, 085403 (2018).
[14] A. Lavasani, D. Bulmash, and S. Das Sarma, Phys. Rev. B **99**, 085104 (2019).
[15] B. Kubala, J. König, and J. Pekola, Phys. Rev. Lett. **100**, 066801 (2008).
[16] B. Dutta, J. T. Peltonen, D. S. Antonenko, M. Meschke, M. A. Skvortsov, B. Kubala, J. König, C. B. Winkelmann, H. Courtois, and J. P. Pekola, Phys. Rev. Lett. **119**, 077701 (2017).
[17] J. Crossno, J. K. Shi, K. Wang, X. Liu, A. Harzheim, A. Lucas, S. Sachdev, P. Kim, T. Taniguchi, K. Watanabe, T. A. Ohki, and K. C. Fong, Science **351**, 1058 (2016).
[18] P. Nozières and A. Blandin, J. Phys. France **41**, 193 (1980).
[19] I. Affleck and A. W. W. Ludwig, Nucl. Phys. B **360**, 641 (1991).
[20] I. Affleck and A. W. W. Ludwig, Phys. Rev. B **48**, 7297 (1993).
[21] P. L. Lopes, I. Affleck, and E. Sela, Phys. Rev. B **101**, 085141 (2020).
[22] R. M. Potok, I. G. Rau, H. Shtrikman, Y. Oreg, and D. Goldhaber-Gordon, Nature (London) **446**, 167 (2007).
[23] A. J. Keller, L. Peeters, C. P. Moca, I. Weymann, D. Mahalu, V. Umansky, G. Zaránd, and D. Goldhaber-Gordon, Nature (London) **526**, 237 (2015).
[24] Z. Iftikhar, S. Jezouin, A. Anthore, U. Gennser, F. D. Parmentier, A. Cavanna, and F. Pierre, Nature (London) **526**, 233 (2015).
[25] V. J. Emery and S. Kivelson, Phys. Rev. B **46**, 10812 (1992).
[26] Z. Iftikhar, A. Anthore, A. K. Mitchell, F. D. Parmentier, U. Gennser, A. Ouerghi, A. Cavanna, C. Mora, P. Simon, and F. Pierre, Science **360**, 1315 (2018).
[27] M. Pustilnik, L. Borda, L. I. Glazman, and J. von Delft, Phys. Rev. B **69**, 115316 (2004).
[28] E. Sela, A. K. Mitchell, and L. Fritz, Phys. Rev. Lett. **106**, 147202 (2011) A. K. Mitchell and E. Sela, Phys. Rev. B **85**, 235127 (2012).
[29] K. A. Matveev, Phys. Rev. B **51**, 1743 (1995) A. Furusaki and K. A. Matveev, *ibid.* **52**, 16676 (1995).
[30] A. K. Mitchell, L. A. Landau, L. Fritz, and E. Sela, Phys. Rev. Lett. **116**, 157202 (2016).
[31] R. Bulla, T. A. Costi, and T. Pruschke, Rev. Mod. Phys. **80**, 395 (2008) A. Weichselbaum and J. von Delft, Phys. Rev. Lett. **99**, 076402 (2007).
[32] R. Kubo, J. Phys. Soc. Jpn. **12**, 570 (1957).
[33] J. M. Luttinger, Phys. Rev. **135**, A1505 (1964).
[34] I. Affleck, A. W. W. Ludwig, H.-B. Pang, and D. L. Cox, Phys. Rev. B **45**, 7918 (1992).
[35] See Supplemental Material at http://link.aps.org/supplemental/10.1103/PhysRevB.102.041111 for a full derivation of Eqs. (7), (8) and (10), and for a discussion on the corrections to the EK point results for finite T/T_K, which includes Refs. [45–48].
[36] A. M. Sengupta and A. Georges, Phys. Rev. B **49**, 10020 (1994).
[37] A. Schiller and S. Hershfield, Phys. Rev. B **58**, 14978 (1998).
[38] D. Bernard and B. Doyon, J. Phys. A **45**, 362001 (2012).
[39] A. K. Mitchell, M. R. Galpin, S. Wilson-Fletcher, D. E. Logan, and R. Bulla, Phys. Rev. B **89**, 121105(R) (2014); K. M. Stadler, A. K. Mitchell, J. von Delft, and A. Weichselbaum, *ibid.* **93**, 235101 (2016).
[40] T. A. Costi, A. C. Hewson, and V. Zlatic, J. Phys.: Condens. Matter **6**, 2519 (1994).
[41] A. Rosch, Eur. Phys. J. B **85**, 6 (2012).
[42] A. K. Mitchell, K. G. L. Pedersen, P. Hedegård, and J. Paaske, Nat. Commun. **8**, 15210 (2017).
[43] M. R. Galpin, A. K. Mitchell, J. Temaismithi, D. E. Logan, B. Béri, and N. R. Cooper, Phys. Rev. B **89**, 045143 (2014).
[44] T. K. T. Nguyen and M. N. Kiselev, Phys. Rev. Lett. **125**, 026801 (2020).
[45] K. Majumdar, A. Schiller, and S. Hershfield, Phys. Rev. B **57**, 2991 (1998).
[46] H. Zheng, S. Florens, and H. U. Baranger, Phys. Rev. B **89**, 235135 (2014).
[47] M. Pustilnik, B. van Heck, R. M. Lutchyn, and L. I. Glazman, Phys. Rev. Lett. **119**, 116802 (2018).
[48] L. A. Landau, E. Cornfeld, and E. Sela, Phys. Rev. Lett. **120**, 186801 (2018).